EPJ Web of Conferences **175**, 05007 (2018) https://doi.org/10.1051/epjconf/201817505007
Lattice 2017

ρ resonance from the $I = 1$ $\pi\pi$ potential in lattice QCD

Daisuke Kawai[1,⋆] for HAL QCD Collaboration

[1] *Department of Physics, Kyoto University, Kyoto 606-8502, Japan*

Abstract. We calculate the phase shift for the $I = 1$ $\pi\pi$ scattering in 2+1 flavor lattice QCD at $m_\pi = 410$ MeV, using all-to-all propagators with the LapH smearing. We first investigate the sink operator independence of the $I = 2$ $\pi\pi$ scattering phase shift to estimate the systematics in the LapH smearing scheme in the HAL QCD method at $m_\pi = 870$ MeV. The difference in the scattering phase shift in this channel between the conventional point sink scheme and the smeared sink scheme is reasonably small as long as the next-to-leading analysis is employed in the smeared sink scheme with larger smearing levels. We then extract the $I = 1$ $\pi\pi$ potential with the smeared sink operator, whose scattering phase shift shows a resonant behavior (ρ resonance). We also examine the pole of the S-matrix corresponding to the ρ resonance in the complex energy plane.

1 Introduction

The understanding of hadron spectra including unstable particles from the first principle is one of the important goals in lattice QCD. Physical observables of unstable particles are measured through two or more stable particle scatterings. Thanks to the advanced numerical techniques such as variational method [1, 2] and all-to-all propagators [3, 4], mesonic unstable particles such as ρ, a_0 and σ are investigated in detail [5–11] with the Lüscher's finite volume method [12] and its extensions [13–15].

An alternative way to investigate unstable particles is the HAL QCD method [17–19], in which scattering phase shifts are calculated from corresponding potentials. For example, the method has been successfully applied to possible exotic hadrons such as Zc(3900) [20]. In this work, we extend the HAL QCD potential method to conventional resonances such as ρ, whose high numerical cost in lattice QCD requires the sink smearing scheme for the HAL QCD potential. In principle, the scattering phase shift is independent of sink operator schemes as long as the potential is evaluated exactly [21]. In practice, however, the truncation of the derivative expansion for the potential introduces some scheme dependences of observables. Therefore, we first investigate the $I = 2$ $\pi\pi$ system, which is easier to handle and has been investigated well. Lessons we obtain are summarized below. (1) The point sink operator scheme, the standard of the HAL QCD potential method, is a good scheme in the sense that the leading order (LO) analysis gives the correct scattering phase shift. (2) The next-to-leading (NLO) analysis is needed for the smeared sink scheme to reproduce the scattering phase shift consistent with the one in the point sink scheme. (3) A sufficiently large number of the smearing level is also required. Otherwise NNLO (or more) analysis would be needed. We then apply the LapH smearing [3, 4] to the $I = 1$ $\pi\pi$ system, in order to extract the corresponding scattering phase shift. As

⋆Speaker, e-mail:daisuke@gauge.scphys.kyoto-u.ac.jp

a number of smearing level increases, a resonant behavior is clearly seen in the scattering phase shift. This is the first time to observe the conventional resonance like ρ in the HAL QCD potential method. We also determine the mass and decay width of the ρ resonance from the pole of the S-matrix in the complex plane.

2 Time-dependent HAL QCD method with the LapH smearing

2.1 Time-dependent HAL QCD method

The main quantity in the HAL QCD method is the Nambu-Bethe-Salpeter (NBS) wave function, which is defined in the $I = 2$ $\pi\pi$ system as

$$\psi^W_{n_s}(\mathbf{r}) = \sum_{\mathbf{x}} \left\langle 0|\pi^-_{n_s}(\mathbf{x},0)\pi^-_{n_s}(\mathbf{x}+\mathbf{r},0)|\pi^-\pi^-, W\right\rangle, \tag{1}$$

where $|0\rangle$ is the QCD vacuum, $|\pi^-\pi^-, W\rangle$ is the $\pi\pi$ eigenstate in the $(I, I_z) = (2, -2)$ channel with the central mass energy W, $\pi^-_{n_s}(x)$ is the negatively charged pion operator, defined by

$$\pi^-_{n_s}(x) = \sum_a \bar{u}^a_{n_s}(x)\gamma_5 d^a_{n_s}(x), \tag{2}$$

where a is the index for color, and the label n_s represents the smearing level, which will be explained in the later subsection.

In the actual calculation of potentials, 2-pt functions

$$C^2_{n_a,n_b}(t,t_0) = \sum_{\mathbf{x},\mathbf{y}} \left\langle \pi^-_{n_a}(\mathbf{x},t)\pi^+_{n_b}(\mathbf{y},t_0)\right\rangle, \tag{3}$$

and 4-pt correlations

$$C^{4,\Lambda,\mu}_{n_a,n_b}(\mathbf{r},t;|\mathbf{P}|,t_0) = \sum_{\mathbf{x}} \left\langle \pi^-_{n_a}(\mathbf{x},t)\pi^-_{n_a}(\mathbf{x}+\mathbf{r},t)(\pi_{n_b}\pi_{n_b})^{\Lambda,\mu}_{2,2}(|\mathbf{P}|,t_0)\right\rangle, \tag{4}$$

are employed. Here n_a and n_b are smearing levels, and the source two pion operator at t_0 is defined as

$$(\pi_{n_s}\pi_{n_s})^{\Lambda,\mu}_{I,I_z}(|\mathbf{P}|,t) = \sum_{\substack{\mathbf{P}\\ |\mathbf{P}|:\text{fix}}} \sum_{I_1,I_2} \sum_{\mathbf{x},\mathbf{y}} C^{\Lambda,\mu}(\mathbf{P}) D^{I,I_z}_{I_1,I_2} e^{-i\mathbf{P}\cdot\mathbf{x}} e^{i\mathbf{P}\cdot\mathbf{y}} \pi^{I_1}_{n_s}(\mathbf{x},t)\,\pi^{I_2}_{n_s}(\mathbf{y},t), \tag{5}$$

with $C^{\Lambda,\mu}(\mathbf{P})$ is the Clebsch-Gordan coefficients in the μ-th component of the irreducible representation Λ of the cubic group, and the relative momentum $\mathbf{P}$ is an element of $\{g\mathbf{P_0}\,|\,g \in O_h, \mathbf{P_0} = [n,0,0]$ in lattice unit with $|\mathbf{P_0}| \le 2\}$, while $D^{I,I_z}_{I_1,I_2}$ is that from two pions with the z component of the isospin I_1 and I_2 to the two pion system with the total isospin I and its z component I_z.

The R-correlator defined as $R^{\Lambda,\mu}_{n_a,n_b}(\mathbf{r},t;|\mathbf{P}|,t_0) \equiv C^{4,\Lambda,\mu}_{n_a,n_b}(\mathbf{r},t;|\mathbf{P}|,t_0)/\left\{C^2_{n_a,n_b}(t,t_0)\right\}^2$ can be decomposed as

$$R^{\Lambda,\mu}_{n_a,n_b}(\mathbf{r},t;|\mathbf{P}|,t_0) = \sum_k A^k_{n_b}\psi^{W_k}_{n_a}(\mathbf{r})e^{-(W_k-2m_\pi)(t-t_0)} + \cdots, \tag{6}$$

where W_k is k-th eigenenergy and ellipses represent inelastic contributions, which become negligible at moderately large t and thus will be neglected in our discussions.

The time-dependent Schrödinger-like equation reads [19]

$$\left(\frac{1}{4m_\pi}\frac{\partial^2}{\partial t^2} - \frac{\partial}{\partial t} - H_0\right) R^{\Lambda,\mu}_{n_a,n_b}(\mathbf{r},t;|\mathbf{P}|,t_0) = \int d^3r'\, U_{n_a}(\mathbf{r},\mathbf{r}')\, R^{\Lambda,\mu}_{n_a,n_b}(\mathbf{r}',t;|\mathbf{P}|,t_0), \tag{7}$$

where the scheme dependence of the potential on the sink operator is explicit as U_{n_a}. It is essential that all elastic states can be used to define the non-local potential $U_{n_a}(\mathbf{r}, \mathbf{r}')$, which, by construction, does not depend on quantities in the source operator such as the relative momentum $|\mathbf{P}|$ and the source smearing level n_b. The ground state saturation is not required any more in this method. In this paper, the non-local potential is approximated at the NLO of the derivative expansion as

$$U_{n_a}(\mathbf{r}, \mathbf{r}') = \left\{ V^{(0)}_{n_a}(r) + V^{(1)}_{n_a}(r)\nabla^2 + O(\nabla^4) \right\} \delta^{(3)}(\mathbf{r} - \mathbf{r}'). \tag{8}$$

We also define effective leading order potential as

$$V^{\mathrm{LO}}_{n_a}(r; |\mathbf{P}|, n_b) \equiv V^{(0)}_{n_a}(r) + V^{(1)}_{n_a}(r) \frac{\nabla^2 R^{\Lambda,\mu}_{n_a,n_b}(\mathbf{r}, t; |\mathbf{P}|, t_0)}{R^{\Lambda,\mu}_{n_a,n_b}(\mathbf{r}, t; |\mathbf{P}|, t_0)}, \tag{9}$$

which may depend on $|\mathbf{P}|$ or n_b unless the second term is negligible.

2.2 LapH smearing

The smeared operator for pion at time t [3, 4] is constructed as

$$\pi^{fg}_{n_s}(\mathbf{x}, t) = \sum_a \bar{q}^{a,f}_{n_s}(\mathbf{x}, t)\gamma_5 q^{a,g}_{n_s}(\mathbf{x}, t) \tag{10}$$

from the smeared quark operator given by

$$q^{a,f}_{n_s}(\mathbf{x}, t) = \sum_{b,\mathbf{y}} \mathcal{S}^{ab}_{n_s}(\mathbf{x}, \mathbf{y}; t) q^{b,f}(\mathbf{y}, t), \tag{11}$$

where $q^{a,f}(\mathbf{x}, t)$ is a local quark field with a color index a and a flavor index f ($f = 1, 2$ for u, d quarks), $\mathcal{S}$ is a smearing operator at time t with smearing level n_s. The maximum number of n_s is given by $L^3 N_c$, where L and N_c are the spatial extent and the number of color, respectively. We denote it as n_{max}. Note that the spinor indices of quarks are implicit and are summed over in the pion operator.

3 Phase shift in the $I = 2$ $\pi\pi$ scattering

We employ the 2+1 flavor gauge configuration on a $16^3 \times 32$ lattice, generated by JLQCD and CP-PACS collaborations with a renormalization-group improved gauge action and non-perturbatively $O(a)$ improved clover action at lattice spacing $a \simeq 0.12$ fm and the pion mass $m_\pi \simeq 870$ MeV [23, 24]. We calculate the potential with point sink and with LapH smeared sink, which we denote *point sink scheme* and *smeared sink scheme*, respectively.

First, let us consider the point sink scheme, in which the smearing level of sink pion operator is set to $n_s = n_{\max}$. This scheme is standard in HAL QCD method. Fig. 1 shows potentials, where source pion operators are constructed with LapH smeared quarks with $n_b = 16$ at $|\mathbf{P}| = 0, 1, 2$ as well as the wall source (denoted as $n_b = 0$) in order to also investigate the source operator dependence. From the figure, it turns out that the potential shows no source momentum dependence and source operator dependence in this scheme, which demonstrate the robustness of the HAL QCD potential at $k \leq 1.4$ GeV.[1]

Next, we discuss the smeared sink scheme with smearing level $n_s < n_{\max}$. In this scheme, we calculate potentials with smearing level $n_s = 64$ and $|\mathbf{P}| = 0, 1$, shown in Fig. 2(a). Unlike the point

[1] It is estimated by $2 \times \frac{2\pi}{La} \sim 1.4$ GeV at $|\mathbf{P}| = 2$.

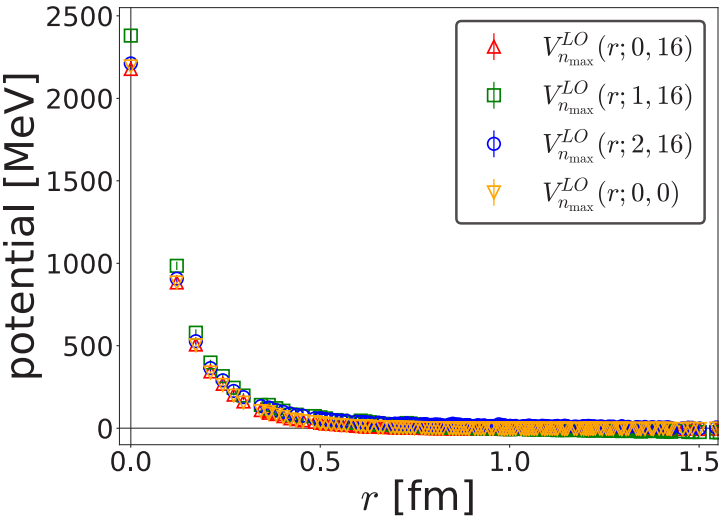

Figure 1. The effective LO potential in the point sink scheme $V^{\rm LO}_{n_{\max}}(r;|\mathbf{P}|,n_b)$ with $n_b = 16$ at $|\mathbf{P}| = 0$ (red up triangles), 1(green squares), 2(blue circles), together with $V^{\rm LO}_{n_{\max}}(r;0,n_b)$ with $n_b = 0$ (orange down triangles) for $I = 2$ $\pi\pi$ scattering.

sink scheme, the potentials in the smeared sink scheme show the sizable momentum dependence, which indicates that $V^{(1)}_{64}$ (or higher order terms) in the derivative expansion is non-negligible. We decompose $V^{\rm LO}_{64}(r;0,64)$ and $V^{\rm LO}_{64}(r;1,64)$ into $V^{(0)}_{64}(r)$ and $V^{(1)}_{64}(r)$ by solving Eq. 9. $V^{(0)}_{64}(r)$ and $V^{(1)}_{64}(r)$ together with $V^{\rm LO}_{64}(r;0,64)$ and $V^{\rm LO}_{64}(r;1,64)$ are shown in Fig. 2(b). Light-blue and yellow bands show fits of $V^{(0)}_{64}$ and $V^{(1)}_{64}$, respectively, where $V^{(0)}_{64}$ is fitted at all r while $V^{(1)}_{64}$ is fitted at $r < 0.8$ fm so as to exclude singular behaviors. Interestingly, $V^{(0)}_{64}(r)$ is almost identical to $V^{\rm LO}_{64}(r;0,64)$. This fact implies that the NLO or higher order terms are negligible at low energy but they become sizable as energy increases. The phase shifts obtained from these potentials as well as $V^{\rm LO}_{n_{\max}}$ are shown in 2(c). While all three cases agree at low energy, they deviate as energy increases. As the NLO analysis is employed for the smeared sink scheme, the agreement with the point sink scheme is improved at higher energies. In order to make a more precise comparison, $k\cot\delta_0$ is shown in Fig. 2(d), where the phase shifts from Lüscher's finite volume method [12] at $k^2 = 7.2\times10^{-3}(^{+13}_{-5})$ GeV^2 and $0.43(^{+1}_{-0})$ GeV^2 are also given. At $k \sim 0$ GeV, while the NLO contribution has a little effect, an increase of smearing level makes an agreement better. On the contrary, the NLO term is vital at $k^2 \simeq 0.43$ GeV^2, suggesting an importance of the NLO analysis at higher energy in the smeared sink scheme.

4 Phase shift in the $I = 1$ $\pi\pi$ scattering and ρ resonance

In this section, we consider the $I = 1$ $\pi\pi$ system, which is known to have the ρ resonance. We employ the 2+1 flavor gauge configuration on a $32^3 \times 64$ lattice, generated by PACS-CS collaboration with a renormalization-group improved gauge action and a non-perturbatively $O(a)$ improved clover quark action at lattice spacing $a \simeq 0.0907$ fm and the pion mass $m_\pi \simeq 410$ MeV [25]. Thanks to the LapH smearing, necessary diagrams for this channel are calculated in affordable cost. Effective LO potentials in the smeared sink scheme in the T_1^- representation at $|\mathbf{P}| = 1$ are shown in Fig. 3 with

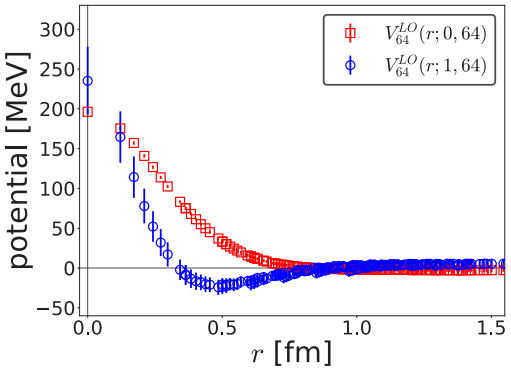

(a) The effective LO potentials in the smeared sink scheme with $n_a = n_b = 64$ at $|\mathbf{P}| = 0$ (red squares) and 1 (blue circles).

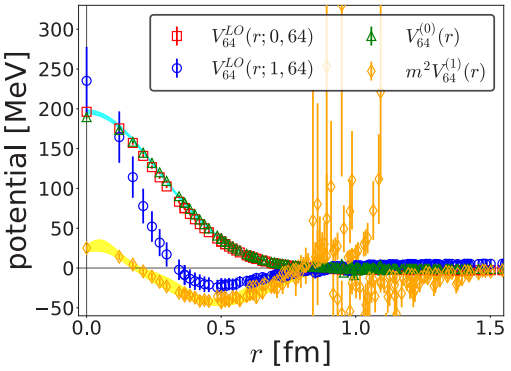

(b) The NLO decomposition, $V_{64}^{(0)}$ (green up triangles) and $V_{64}^{(1)}$ (orange diamonds), in the smeared sink scheme with $n_a = n_b = 64$, together with the V_{64}^{LO} at $|\mathbf{P}| = 0$ (red squares) and 1 (blue circles).

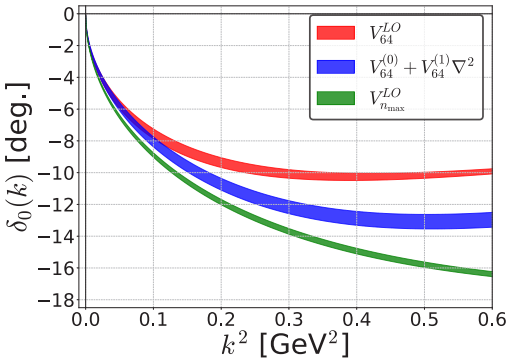

(c) The phase shifts obtained from V_{64}^{LO} (red) and $V_{64}^{(0)} + V_{64}^{(1)}\nabla^2$ (blue) as well as $V_{n_{\max}}^{\mathrm{LO}}$ (green).

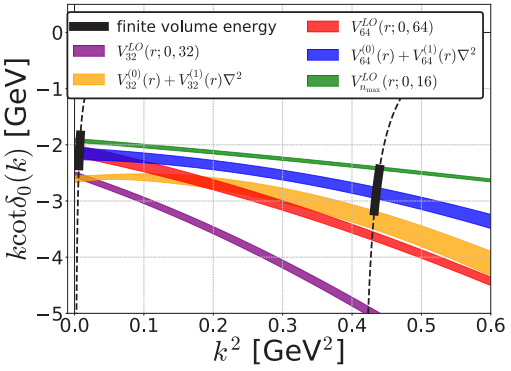

(d) $k\cot\delta_0$ obtained from $V_{64}^{(0)} + V_{64}^{(1)}\nabla^2$ (blue), $V_{32}^{(0)} + V_{32}^{(1)}\nabla^2$ (yellow), and $V_{n_{\max}}^{\mathrm{LO}}$ (green), together with V_{64}^{LO} (red) and V_{32}^{LO} (purple), as well as those from the finite volume method (bold black bands).

Figure 2. Potentials and phase shifts in the smeared sink scheme for $I = 2$ $\pi\pi$ scattering

$n_a = 64$ and 128, where some data with exceptionally large statistical error which come from nodes (zeros of the R-correlator) are omitted. In contrast to the $I = 2$ system, both potentials show attractive behaviors with the 2 GeV depth at the origin for $n_a = 128$. Scattering phase shifts obtained from $V_{64}^{\mathrm{LO}}(r;0,64)$ and $V_{128}^{\mathrm{LO}}(r;0,128)$ as well as those obtained from the Lüscher's finite volume method on the same ensemble by PACS-CS collaboration [26] are shown in Fig. 4. As the smearing level increases from $n_a = 64$ (blue down triangle) to $n_a = 128$ (red up triangles), the scattering phase shift sharply increases at $\sqrt{s} \equiv 2\sqrt{m_\pi^2 + k^2} \simeq 850$ MeV and reaches 90 degrees at $\sqrt{s} \simeq 910$ MeV, suggesting an existence of the ρ resonance state in this energy region. It is the first demonstration that the HAL QCD potential describes the conventional resonance such as ρ. We note, however, that the discrepancies between $n_a = 128$ and 64 indicate that the NLO term in the derivative expansion is not negligible at higher energies, as was observed in the smeared sink scheme for I=2 channel. In fact, the

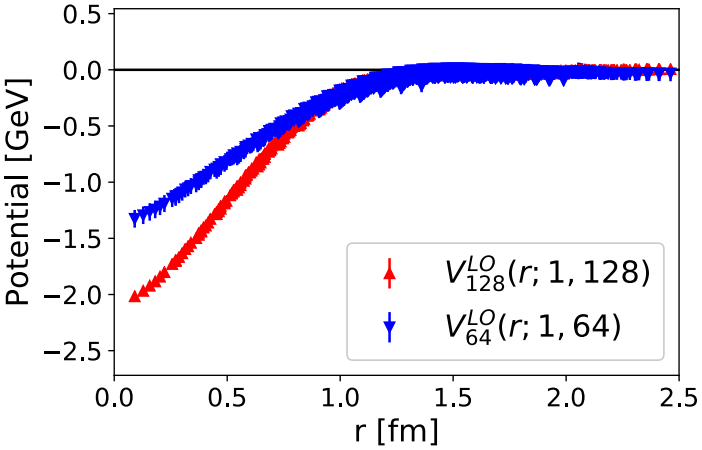

Figure 3. The effective LO potential in the smeared sink scheme $V^{\rm LO}_{n_a}(r;|\mathbf{P}|,n_b)$ with $n_a = n_b = 128$ (red up triangles) and 64 (blue down triangles) for $I = 1$ $\pi\pi$ scattering.

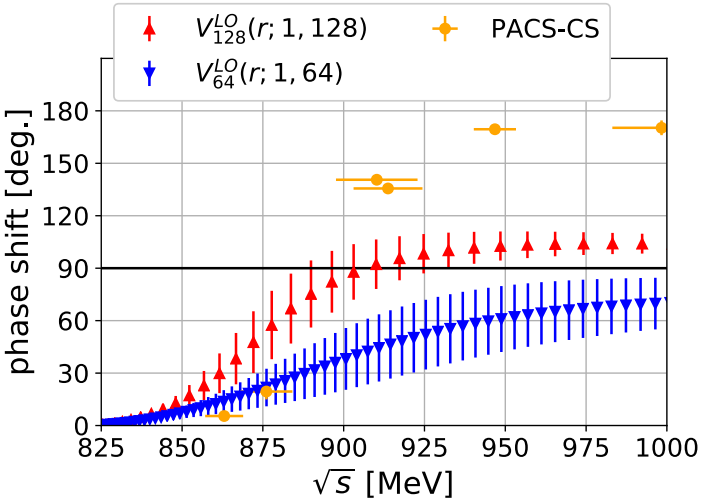

Figure 4. The phase shifts obtained from $V^{\rm LO}_{128}(r;1,128)$ (red up triangles) and $V^{\rm LO}_{64}(r;1,64)$ (blue down triangles), together with those by Lüscher's finite volume method on the same configuration (orange circles).

phase shift stops rising at $\sqrt{s} \simeq 950$ MeV, so that it deviates from the finite volume results by PACS-CS collaboration (orange circles). In future studies, we should further increase the smearing level n_a, together with the NLO analysis, which requires data at $|\mathbf{P}| > 1$, in order to control the systematic uncertainties of the scattering phase shift at higher energies.

The HAL QCD potential allows us to determine mass and decay width of the resonance state, without using the fit ansatz such as the Breit-Wigner form. If a potential dumps exponentially at long

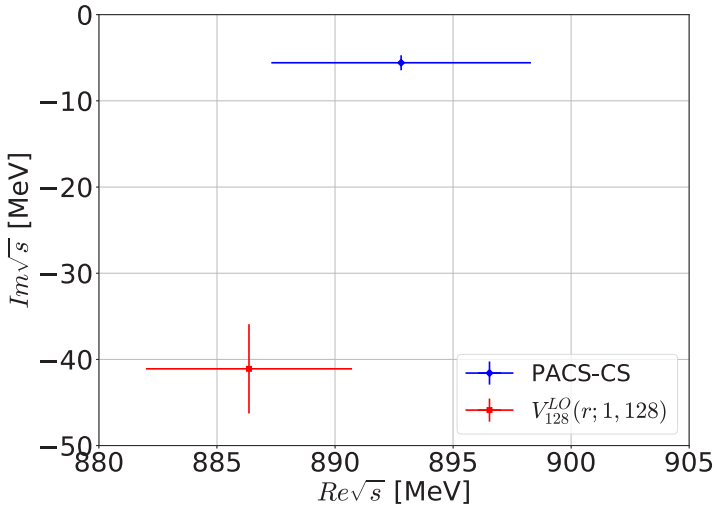

Figure 5. The pole position from the direct pole search with $V_{128}^{\mathrm{LO}}(r;1,128)$ (red), compared with the Breit-Wigner pole by PACS-CS collaboration (blue).

distance, Schrödinger equation

$$\left(\frac{k^2}{m_\pi} - H_0\right)\psi_{n_a,n_b}^{T_1,\mu}(\mathbf{r},t) = V_{n_a}^{\mathrm{LO}}(\mathbf{r};|\mathbf{P}|,n_b)\,\psi_{n_a,n_b}^{T_1,\mu}(\mathbf{r},t), \tag{12}$$

can be analytically continued to the complex k-plane as $k \to ke^{i\theta}$ and $r \to re^{-i\theta}$ [27–29], where $\psi_{n_a,n_b}^{T_1,\mu}$ is a NBS wave function and $\theta \in \mathbb{R}$. We denote the radial part of $\psi_{n_a,n_b}^{T_1,\mu}$ for orbital angular momentum L as $\phi_L^{T_1,\mu}$. At $r \gg 1$, It is given by

$$\phi_L^{T_1,\mu}(r,t) \sim \frac{i}{2}\left(\mathcal{J}_L(+k)h_L^-(kr) - \mathcal{J}_L(-k)h_L^+(kr)\right), \tag{13}$$

where $\mathcal{J}_L$ and $h_L^\pm$ are Jost function and Riccati-Hankel functions, respectively. Changing k and θ, we search for the pole position of S-matrix $s_{l=1}(k) = \mathcal{J}_1(-k)/\mathcal{J}_1(k)$, which gives the resonance mass and decay width, shown in Fig. 5. The mass from the potential is consistent with the finite volume result, though the width is about eight times larger due to the smearing. Future studies mentioned before will be needed to improve the determination of the pole position.

5 Conclusion

We calculated the scattering phase shift for $I = 1, 2$ $\pi\pi$ systems form the HAL QCD potential with the LapH smearing.

It has been shown for the $I = 2$ $\pi\pi$ scattering that truncation errors of the derivative expansion in the smeared sink scheme are under controll by the NLO analysis with larger smearing levels.

Preliminary results for the $I = 1$ $\pi\pi$ scattering phase shift show the resonant behavior, though analyses with increased smearing level and/or higher order terms in the derivative expansion are necessary to quantify the systematic uncertainties. We then determine the pole position of the ρ resonance in the complex plane. Although future improvements will be required, our study demonstrates that the HAL QCD method can be used to study resonance states as well.

6 Acknowledgement

D.K. is supported in part by the Japan Society for the Promotion of Science (JSPS). We thank the JLQCD collaboration, CP-PACS collaboration and PACS-CS collaboration for providing us their 2+1 flavor gauge configurations [23–25]. The code for the eigenvectors of gauge covariant Laplacian was supplied by Prof. C. Morningstar. We fairly thank for his kindness. Numerical calculations in this study have been performed on XC40 at YITP in Kyoto University and BlueGene/Q in KEK (Nos. 15/16-12).

References

[1] M. Lüscher and U. Wolff, Nucl. Phys. B339, 222 (1990).
[2] C. Michael, Nucl. Phys. B 259, 58 (1985).
[3] M. Peardon et al., (Hadron Spectrum Collaboration), Phys. ReV. D 80, 054506 (2009).
[4] C. Morningstar et al., Phys. ReV. D 83, 114505 (2011).
[5] J. J. Dudek, R. G. Edwards, and C. E. Thomas, (for the Hadron Spectrum Collaboration), Phys. ReV. D 87, 034505 (2013).
[6] C. Helmes et al., arXiv[hep-lat]:1512.00282
[7] R. A. Briceño, J. J. Dudek, R. G. Edwards, D. J. Wilson (for the Hadron Specturm Collaboration), Phys, Rev, Lett. 118, 022002 (2017).
[8] L. Liu et al. (ETM Collaboration), arXiv[hep-lat]: 1612.02061.
[9] R. A. Briceño, J. J. Dudek, R. G. Edwards, and D. J. Wilson (for the Hadron Specturm Collaboration), arXiv[hep-lat]:1708.06667
[10] R. A. Briceño et al., (for the Hadron Spectrum Collaboration), Phys. Rev. D 93,094506 (2016).
[11] Zhi-Hui Guo et al. Phys. Rev. D 95, 054004 (2017).
[12] M. Lüscher, Nucl. Phys. B 354 531 (1991).
[13] K. Rummukainen and S. Gottlieb, Nucl. Phys. B450 (1995) 397-436
[14] P. Guo, J. Dudek, R. Edwards, A. P. Szczepaniak Phys. Rev. D 88, 014501 (2013)
[15] S. He, X. Feng, C. Liu, JHEP 0507, 011 (2005).
[16] R. A. Briceño and Z Davoudi, Phys. Rev. D 88, 094507 (2013)
[17] N. Ishii, S. Aoki and T. Hatsuda, Phys. ReV. Lett. 99, 022001 (2007).
[18] S. Aoki, T. Hatsuda and N. Ishii, Prog. Theor. Phys. 123, 89 (2010).
[19] N. Ishii et. al. (HAL QCD Collaboration), PLB 712 (2012) 437.
[20] Y. Ikeda et al, (HAL QCD Collaboration), Phys. Rev. Lett. 117, 242001 (2016).
[21] S. Aoki et al. (HAL QCD Collaboration), Prog. Theor. Exp. Phys. 2012, 01A105 (2012)
[22] C. Morningstar and M. J. Peardon, Phys. Rev. D69, 054501 (2004).
[23] S. Aoki et al., (JLQCD Collaboration), Phys. Rev. D 65 (2002).
[24] T. Ishikawa et al., (CP-PACS, JLQCD Collaboration), Phys. Rev. D 73 (2006)
[25] S. Aoki et al., (PACS-CS Collaboration), Phys. Rev. D 79:034503,2009
[26] S. Aoki et al., (PACS-CS Collaboration), Phys. Rev. D 84(2011)094505
[27] B.G. Giraud, K. Kato amd A. Ohnishi, J. Phys. A 37 (2004)11575
[28] J. Aguilar and J.M. Combes, Commun. Math. Phys.,22 (1971) 269
[29] E. Balslev and J.M. Combes, Commun. Math. Phys.,22 (1971) 280